OncoImmunology

ISSN: (Print) (Online) Journal homepage: https://www.tandfonline.com/loi/koni20

Anti-Ly6G binding and trafficking mediate positive neutrophil selection to unleash the anti-tumor efficacy of radiation therapy

Gaël Boivin, Pierre-Benoit Ancey, Romain Vuillefroy de Silly, Pradeep Kalambaden, Caroline Contat, Benoit Petit, Jonathan Ollivier, Jean Bourhis, Etienne Meylan & Marie-Catherine Vozenin

To cite this article: Gaël Boivin, Pierre-Benoit Ancey, Romain Vuillefroy de Silly, Pradeep Kalambaden, Caroline Contat, Benoit Petit, Jonathan Ollivier, Jean Bourhis, Etienne Meylan & Marie-Catherine Vozenin (2021) Anti-Ly6G binding and trafficking mediate positive neutrophil selection to unleash the anti-tumor efficacy of radiation therapy, OncoImmunology, 10:1, 1876597, DOI: 10.1080/2162402X.2021.1876597

To link to this article: https://doi.org/10.1080/2162402X.2021.1876597

ONCOIMMUNOLOGY
2021, VOL. 10, NO. 1, e1876597 (12 pages)
https://doi.org/10.1080/2162402X.2021.1876597

Taylor & Francis
Taylor & Francis Group

ORIGINAL RESEARCH

OPEN ACCESS Check for updates

Anti-Ly6G binding and trafficking mediate positive neutrophil selection to unleash the anti-tumor efficacy of radiation therapy

Gaël Boivin[a,b,c], Pierre-Benoit Ancey[b], Romain Vuillefroy de Silly[d], Pradeep Kalambaden[a], Caroline Contat[b], Benoit Petit[a,c], Jonathan Ollivier[a,c], Jean Bourhis[a,c], Etienne Meylan[b], and Marie-Catherine Vozenin[a,c]

[a]Radio-Oncology Laboratory, Department of Oncology, Lausanne University Hospital and University of Lausanne, Lausanne, Switzerland; [b]School of Life Sciences Ecole Polytechnique Fédérale De, Lausanne, Swiss Institute for Experimental Cancer Research, Lausanne, Switzerland; [c]Radio-Oncology Service, Department of Oncology, Lausanne University Hospital and University of Lausanne, Lausanne, Switzerland; [d]The Ludwig Institute for Cancer Research, University of Lausanne, Epalinges, Switzerland

ABSTRACT

The anti-Ly6G antibody is used to deplete Ly6G^{pos} neutrophils and study their role in diverse pathologies. However, depletion is never absolute, as Ly6G^{low} neutrophils resistant to depletion rapidly emerge. Studying the functionality of these residual neutrophils is necessary to interpret anti-Ly6G-based experimental designs. *In vitro*, we found anti-Ly6G binding induced Ly6G internalization, surface Ly6G paucity, and primed the oxidative burst of neutrophils upon TNF α co-stimulation. *In vivo*, we found neutrophils resistant to anti-Ly6G depletion exhibited anti-neutrophil-cytoplasmic-antibodies. In the pre-clinical *Kras$^{Lox\text{-}STOP\text{-}Lox\text{-}G12D/WT}$; Trp53$^{Flox/Flox}$* mouse lung tumor model, abnormal neutrophil accumulation and aging was accompanied with an N2-like SiglecF^{pos} polarization and *ly6g* downregulation. Consequently, SiglecF^{pos} neutrophils exposed to anti-Ly6G reverted to Ly6G^{low} and were resistant to depletion. Noting that anti-Ly6G mediated neutrophil depletion alone had no anti-tumor effect, we found a long-lasting rate of tumor regression (50%) by combining anti-Ly6G with radiation-therapy, in this model reputed to be refractory to standard anticancer therapies. Mechanistically, anti-Ly6G regulated neutrophil aging while radiation-therapy enhanced the homing of anti-Ly6G-boundSiglecF^{neg} neutrophils to tumors. This anti-tumor effect was recapitulated by G-CSF administration prior to RT and abrogated with an anti-TNFα antibody co-administration. In summary, we report that incomplete depletion of neutrophils using targeted antibodies can intrinsically promote their oxidative activity. This effect depends on antigen/antibody trafficking and can be harnessed locally using select delivery of radiation-therapy to impair tumor progression. This underutilized aspect of immune physiology may be adapted to expand the scope of neutrophil-related research.

ARTICLE HISTORY
Received 8 September 2020
Revised 11 January 2021
Accepted 12 January 2021

KEYWORDS
Anti-neutrophil cytoplasmic antibody (ANCA); depletion resistance; tumor-associated-neutrophils (TANs) polarization; radio-sensitization

Introduction

The anti-Ly6G antibody (ab) has been widely used to deplete neutrophils and investigate their role in malignancies.[1–6] However, this strategy suffers limitations: the depletion efficacy of anti-Ly6G is partial, transient, and neutrophil numbers rebound as soon as 3 d after treatment initiation.[7] The mechanism involved in this rebound or resistance to depletion is unclear, but seems independent from schedule of treatment[7] or from the occurrence of abs against the anti-Ly6G ab.[7] Enhanced granulopoiesis was further proposed as a depletion resistance mechanism, but the transient efficacy of anti-Ly6G has also been shown in granulocyte colony-stimulating factor (G-CSF)-driven models, [5] suggesting that resistance could be dependent upon an adaptative process. Recently, we reported that neutrophils silence ly6g under physiological condition as they exit from the bone marrow (BM) and that neutrophils resistant to anti-Ly6G depletion had low surface expression of Ly6G .[8]

In cancer studies, partial or transient neutrophil depletion complicates the interpretation of results, as cancer models require several weeks of antibody-treatment and follow-up.[9] The biological significance of residual and anti-Ly6G bound neutrophils has not been investigated. However, clinical pathologies, such as transfusion-related acute lung injury, [10] and granulomatosis polyangiitis ;[11] where antibodies targeting the membrane of neutrophils and anti-neutrophil cytoplasmic antibodies (ANCAs) are, respectively, found; suggest that antibody-targeted neutrophils can be harmful, especially to lung tissues. Whether this latter feature might be used to enhance the efficacy of anti-cancer treatment has not been envisaged previously.

Neutrophilia after radiation therapy (RT) translates to poor clinical outcome.[1,12–15] These correlative studies are mostly based on blood neutrophil analysis, but the physiology of tumor-associated-neutrophils (TANs) after RT requires further investigation. The *KrasLox-STOP-Lox-G12D/WT; Trp53$^{Flox/Flox}$* (KP) non-small-cell lung cancer (NSCLC)

CONTACT Marie-Catherine Vozenin marie-catherine.vozenin@chuv.ch Radio-Oncology Laboratory, Department of Oncology, Lausanne University Hospital and University of Lausanne, Lausanne, Switzerland.
Supplemental data for this article can be accessed on the publisher's website.

model mimics the natural course of human adenocarcinoma.[16] KP-tumor infiltrating myeloid cells, including TANs, are conserved across individuals and mouse/human species, [17] according to a single-cell RNAseq analysis publically available.[17] High KP-TAN prevalence was shown to correlate with KP-tumor progression.[2] Treatment with the anti-Gr1 ab, which recognizes both Ly6C and Ly6G antigens (ags), reduced KP-TAN prevalence by 70%, slowed KP-tumor growth but did not induce tumor regression.[2,3] A N2-like subset of SiglecF^{Pos} TANs with a tumor-associated transcriptomic profile has recently been described and shown to arise from a tumor-induced specific ontogeny.[3,18] Additionally, TANs transiently dominated the microenvironment of KP-tumors after RT.[19] KP-tumors have been shown to be refractory to various anti-cancer treatment including RT; whole thorax irradiation (WTI) with a single dose of 15.5Gy[20] and single-nodule stereotactic irradiation at 2 × 8.5Gy[21] comparably slowed KP-tumor growth down, but did not induce any tumor regression. In KPs, several tumors arise asynchronously and their immune microenvironment display strong intra-inter individual heterogeneity.[2,3,22] Therefore, radiological evaluation has been used in those studies to monitor the growth of single nodules to avoid histological section plan biases.[2,3] In a KP-sarcoma model, anti-Ly6G administration prior to RT enhanced its efficacy, but did not result in tumor regression.[1]

We investigated the intrinsic effect of anti-Ly6G binding on residual neutrophil physiology. Based on our data, we propose that anti-Ly6G/Ly6G internalization along with the presence of ANCA, respectively, act as a resistance mechanism to anti-Ly6G-mediated depletion; and as an intrinsic signal for TNFα-mediated cytotoxic oxydative burst. Using the treatment-resistant KP model, we report that an anti-Ly6G ab exhibits synergy with RT to achieve a 50% partial KP-tumor regression rate in a TNFα-dependent manner, in absence of neutrophil depletion. This novel proposed function of anti-Ly6G ab treatments bring into question previous interpretations of neutrophil depletion (reviewed in *24*) and opens some exciting new opportunities to study and manipulate neutrophil function.

Results

Anti-Ly6G ab is rapidly internalized in vitro

We used the imagestream technology to track the anti-Ly6G-PE ab localization after binding. BM neutrophils were incubated in cytochalasin D to block cytoskeleton prior anti-Ly6G staining (Figure 1(a)). We observed 4 PE distribution patterns: 1) membrane diffuse; 2) membrane condensation; 3) intra-cellular condensation; 4) diffuse intracellular (Figure 1(b)). After 1 hour of binding, 80% of neutrophils showed anti-Ly6G-PE internalization *versus* 20% of them if cytoskeleton was chemically inhibited (Figure 1(c)). PE signal colocalizing with membrane CD45 inversely varied (Figure 1(d)). A less sensitive additional methodology, using fluoro-labeled anti-rat antibody to detect the rat anti-Ly6G ab, validated this point (Fig. S1a-f).

Anti-Ly6G ab generates ANCAs in vivo

We treated mice C57Bl6 mice with anti-Ly6G ab for 5 d and tracked its distribution *in vivo*. Despite daily treatment with anti-Ly6G, neutrophil prevalence was not affected in BM, blood and lung (Figure 1(e-f)). As we previously reported, adult C57Bl6 mice background is refractory to neutrophil depletion as newly synthesized Ly6G^{low} neutrophils reconstitute the pool of circulating neutrophils as early as 1 d after treatment initiation.[8] We then characterized the anti-Ly6G ab localization in the cell with imagestream. In anti-Ly6G treated cells, we found, respectively, 25% and 90% of BM and blood neutrophils exhibiting cytosolic anti-Ly6G ab (Figure 1(g-i)). Additionally, on cytospined BM cells, we observed a colocalization of the *in vivo* delivered anti-Ly6G ab with calnexin, an endoplasmic reticulum protein. Despite an ethanol fixation, the distribution of the *in-vivo* delivered anti-Ly6G was cytosolic and not peri-nuclear. We conclude anti-Ly6G generates cytoplasmic-ANCA (c-ANCA) *in vivo*. Our setting was not adapted to determine whether anti-Ly6G entered the cytosol directly through membrane pores *in vivo*, or if it leaked from endosomes to the cytosol after internalization.

The Ly6G/anti-Ly6G complex internalization is a depletion resistance mechanism

The expression of Ly6G on the surface of neutrophils increases as they mature.[23] Accordingly, the mean fluorescence intensity (MFI) for Gr1 (that recognizes the Ly6G ag despite previous anti-Ly6G binding) in blood neutrophils was higher than in BM (Figure 2(a)). However, in anti-Ly6G treated mice, blood neutrophils had a lower Gr1 MFI than BM neutrophils, suggesting an active loss of the Ly6G ag during/after they exit from the BM (Figure 2(a)). Moreover, TNF α exposure enhanced Ly6G translocation to the membrane (Figure 2(a)) and partially rescued the Gr1 MFI loss in anti-Ly6G treated BM-neutrophils, but not those in blood (Figure 2(a)). Since ly6g is downregulated at the RNA level when neutrophils exit from the BM, [8] we hypothesized that neutrophils may exhibit lower levels of Ly6G protein on the membrane when internalization exceeds translocation of Ly6G. Since the anti-Gr1 ab also recognizes Ly6C, we confirmed that there were no differences in Ly6C expression (Figure 2(b)). Since anti-Ly6G and anti-Gr1 are pauci-competitive (Fig. S2a-g), we implemented our recently published method[8] to stain Ly6G in a specific and sequential manner. This approach confirmed that neutrophils treated with anti-Ly6G were Ly6G^{low} both at the membrane and intracellular levels (Fig. S2h-k). Control experiments using CD11b, another membrane marker of neutrophil maturation, showed no changes in its level of expression (Fig. S2l.m). In conclusion, anti-

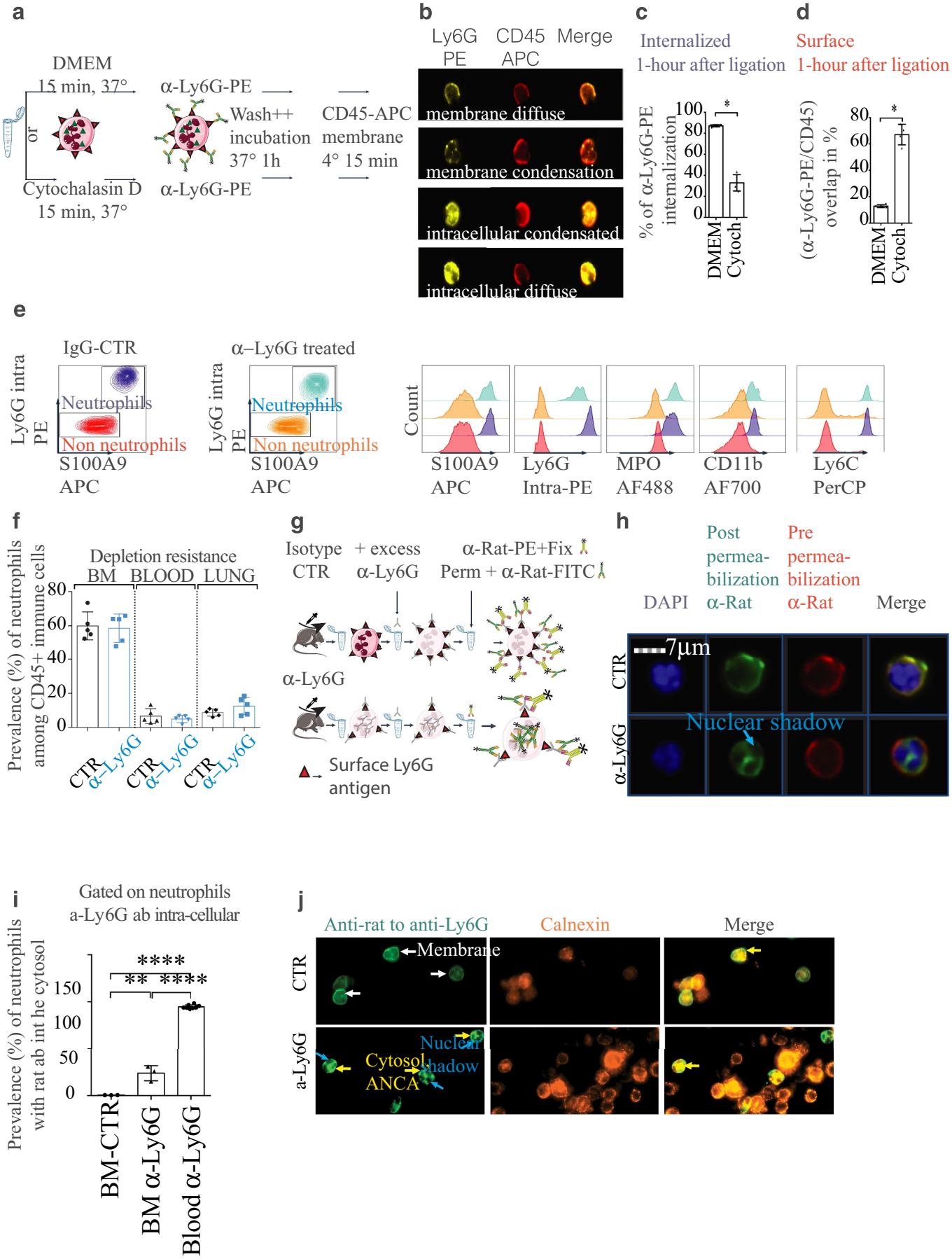

Figure 1. Neutrophils resistant to anti-Ly6G depletion exhibit ANCAs. (a). Ly6G binding and trafficking: untreated BM cells were incubated with DMEM or cytochalasin D before anti-Ly6G-PE staining. After 1 hour of incubation, bone marrow (BM) cells were stained with CD45-APC. (b). Representative images obtained with imagestream

to localize Ly6G-PE. (c.d). Quantification from b (n = 3 DMEM, n = 4 Cytochalasin D, 500 neutrophils/sample). (e) Gated on immune cells. Sensitive strategy based on S100A9 and intra-cellular Ly6G staining to detect neutrophils after anti-Ly6G treatment. Note that only the MFI for intra-cellular Ly6G is lower in anti-Ly6G treated mice. f Neutrophil prevalence quantification in BM, blood and lungs after 5 d of isotype CTR or anti-Ly6G treatment (n = 5 mice per group, 25 µg of ab, daily). g. Scheme of experiment to track anti-Ly6G delivered in-vivo after 5 d of treatment (25 µg of ab, daily). Excess unlabeled anti-Ly6G (200 ml at 10µ g/mL for 15 minutes) is added prior fixation to allow CTR cell detection with an anti-rat-FITC. h. Imagestream images obtained from g are compatible with anti-neutrophil cytoplasmic antibodies (ANCAs) in BM neutrophils. Neutrophils were gated on the basis of the FITC positive signal: note that both anti-rat antibodies are polyclonal and displayed no competition at the surface membrane. DAPI stained nucleus shows several segmentations, which confirms the granulocytic nature of gated cells. (i) Quantification of the intracellular presence of anti-Ly6G ab after 5 d of treatment in the BM, or 1 hour of treatment in the blood (the blood endpoint was added from an additional experiment).j Representative illustration on projected BM cells showing the in-vivo delivered anti-Ly6G colocalizes with calnexin, an endoplasmic reticulum protein).* p < .05, ** p < .01, *** p < 0,001, **** p < 0,0001 from Mann-Whitney test; error bars represent s.d.

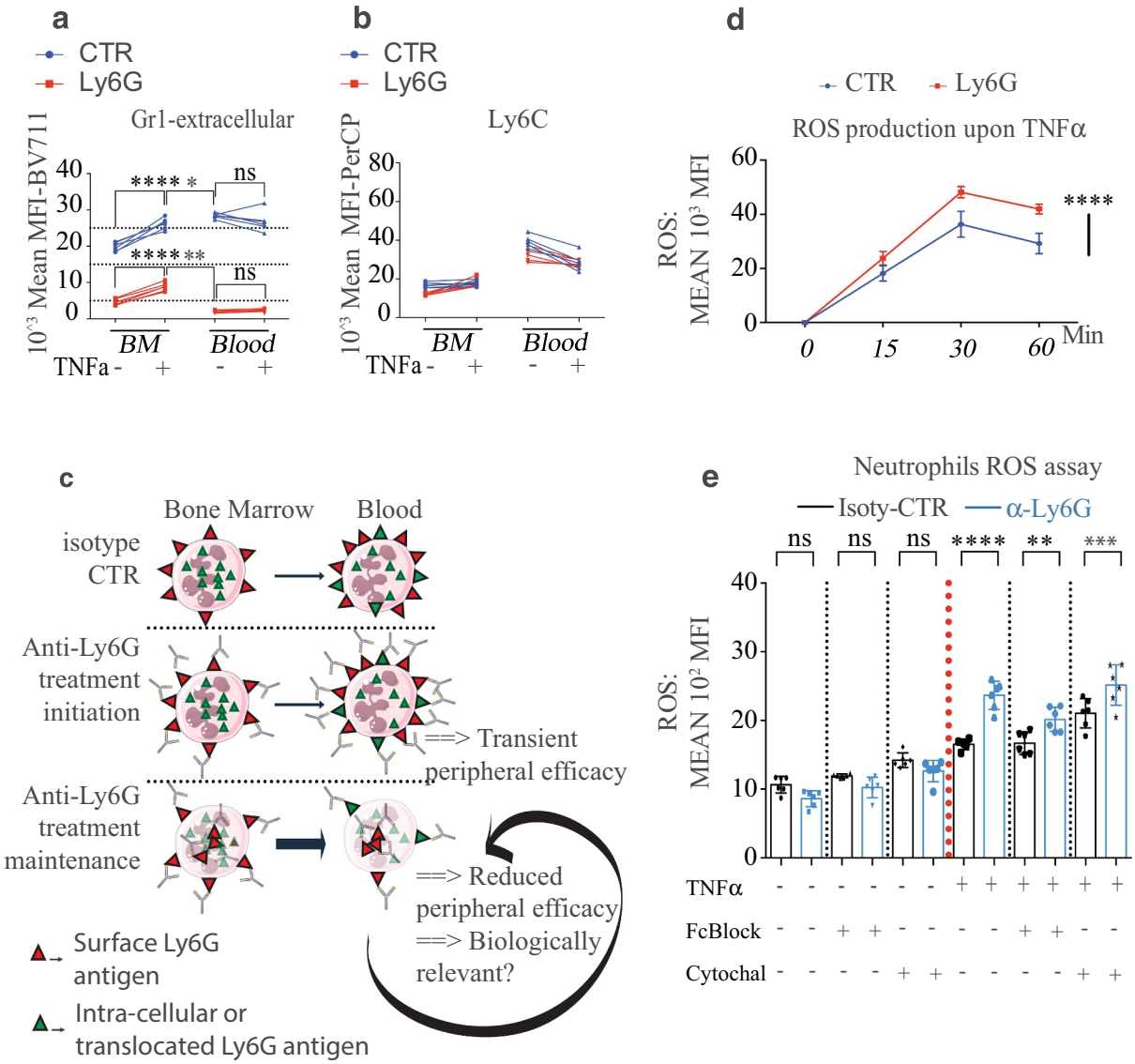

Figure 2. Anti-Ly6G ligation enhances TNFα-induced neutrophil oxidative burst. (a-b). Five mice were treated with anti-Ly6G or isotype CTR for 5 d. Bone marrow (BM) and blood cells were collected and incubated with or without TNFα for 1 hour at 37°C. Cells were subsequently stained with the pauci-competitive anti-Gr1at the surface a and Ly6C (b). Note that the surface levels for Gr1 in the blood neutrophils are lower than levels in the BM, while the neutrophil exit in physiological conditions normally goes with an increase of surface Ly6G, suggesting an active loss of the Ly6G antigen upon in vivo anti-Ly6G treatment p < .05, ** p < .01, *** p < 0,001, **** p < 0,0001 from Mann-Whitney test; error bars represent s.d. (c). Schematic representation of the Ly6G membrane availability upon anti-Ly6G after treatment induction and maintenance. (d). 200000 BM cells were incubated with anti-Ly6G for 15 minutes at 4°C (or isotype CTR, 10 µg/mL), extensively washed, pulsed with TNFα (5 ng/mL) for 30 min at 37°C, and incubated with a ROS detecting probe for 0–15-30 or 60 minutes (n = 6 per group per endpoint). **** p < 0,0001 from 2way ANOVA test; error bars represent s.d e. The experimental setting from d was reproduced for the endpoint 15 min, in the presence of PBS, FcBlock or Cytochalasin D to evaluate the role of residual surface Fc-FcGr interactions as well as the internalization of the Ly6G/anti-Ly6G complex on the enhanced ROS production. Six bone marrows coming from six untreated mice were used. Each bone marrow is divided to test all conditions. treatment p < .05, ** p < .01, *** p < 0,001, **** p < 0,0001 from ANOVA test with multiple comparison; error bars represent s.d

Ly6G ab physically triggers depletion resistance via Ly6G internalization that limits its functional recognition (Figure 2(c)).

Anti-Ly6G binding potentiates TNF α- mediated oxidative burst

Next, we investigated whether the process of antigen/antibody (Ag/Ab) binding and intracellular trafficking were able to modify neutrophil biology (Figure 2(c)). We incubated neutrophils with or without anti-Ly6G for 15 minutes and stimulated them with TNFα. Anti-Ly6G treatment increased reactive oxygen species (ROS) production in both onset and intensity after TNFα stimulation (Figure 2(d)). Both Fc-receptor blockade and cytoskeleton inhibition with cytochalasin D limited the relative increase in TNF α-induced ROS (Figure 2(e)), suggesting that anti-Ly6G binding and trafficking primes the cytotoxic oxidative function of neutrophils under TNFα stimulation.

In summary, we found anti-Ly6G binding at the neutrophil surface-induced internalization of the Ag/Ab complex causing subsequent resistance to depletion. We also report in the present study that anti-Ly6G produced ANCAs. We characterized the phenotype of the residual neutrophils as Ly6G^{low} and found a potentiation of their cytotoxic function with an enhanced capacity to produce ROS upon a pro-inflammatory stimulus. With this new information, we sought to validate the relevance of these findings using a KP NSCLC model, where the neutrophil contribution in modulating tumor response has been well documented.

TAN aging in KP mice is associated with SiglecF+ differentiation

First, we characterized TANs in KP tumors with a specific focus on their lifespan and kinetics of infiltration, since we previously reported anti-Ly6G reduces the longevity of neutrophils.[8] After a single-injection of BrdU (Figure 3(a)), we found that CD11b^{high} Ly6C^{int} Ly6G^{high} F4/80^{neg} SSCa^{low} neutrophils started to infiltrate tumors 60-hours after BrdU incorporation. Following BrdU injection, BrdU+ TANs were detected up to 10 d afterward (Figure 3(b)). While 50% of TANs expressed SiglecF (Figure 3(c)), none of the young (60-hour) infiltrating neutrophils expressed SiglecF (Figure 3(d)). From day 6, the prevalence of BrdU among the SiglecF^{neg} TANs declined while reaching a transient plateau in SiglecF^{pos} TANs. At 10 d after BrdU injection, the rare remaining BrdU+ TANs were exclusively SiglecF^{pos} (Figure 3(d)). Additional markers and histological analyses confirmed those results and excluded an eosinophil contamination (Fig. S3). Thus, we conclude that TANs have an aberrantly long lifespan and that they locally differentiate toward N2-like SiglecF^{pos} cells in a time-dependent manner. We next evaluated the effect of anti-Ly6G delivery on these TAN populations.

Anti-Ly6G treatment gives rise to Ly6G negative TANs

The occurrence of Ly6G negative MDSCs has been reported after anti-Ly6G treatment (reviewed in[24]). The existence of these cells is controversial as they were proposed to result from a Ly6G ag masking issue.[24] To clarify this point and evaluate the efficacy of neutrophil depletion in KPs, we used intracellular staining for Ly6G to circumvent membrane masking, and S100A9 as an additional neutrophil marker, to investigate this further (Figure 3(f)). In untreated KP-TANs, flow cytometry revealed that SiglecF^{high} and SiglecF^{neg} TANs had comparable cell surface levels of Ly6G. Additionally, S100A9 was specific and sensitive for identification of TANs and neutrophils (Figure 3(g)). Upon anti-Ly6G treatment, intracellular staining for Ly6G resolved any potential confounding effects of ag masking and was sufficient to detect neutrophils in BM, blood, and lung tissues, despite reduced MFI Ly6G signal (Figure 3(e-f)). However, the Ly6G ag was lost in SiglecF^{pos} TANs after anti-Ly6G treatment (Figure 3(g)), suggesting that 70% of SiglecF^{pos} TANs are no longer detectable with the Ly6G epitope after anti-Ly6G treatment. This loss of Ly6G expression may reflect an uncompensated Ly6G degradation after antibody binding, since SiglecF TANs were reported as ly6g low at the RNA level (Figure 3(h) adapted from an available online database[17]).

Antibody-mediated TAN depletion is limited and exhibits no anti-tumor effect

We challenged KP mice with three antibody-based neutrophil depletion strategies (Anti-Gr1, Anti-Ly6G, Anti-Ly6G +Mar18.5) and monitored tumor response with unbiased CT-scan imagery. Consistent with previous studies, [2,21,25] untreated KP-tumors grew 2.3 fold in 2 weeks (Figure 4(b-d)). Anti-Gr1-reduced TAN prevalence and decreased tumor growth by 35% in the absence of regression (Figure 4(b,c)). Anti-Ly6G failed to reduce TAN prevalence and did not affect tumor growth (Figure 4(b,c)). Anti-Gr1 is less specific than anti-Ly6G, as it recognizes Ly6C, but was more efficient than anti-Ly6G to reduce TAN prevalence (Figure 4(b,c)). To discriminate between these two variables, we used a recent strategy involving anti-Ly6G+anti-Rat-Mar18.5 to reduce TAN prevalence comparably to anti-Gr1.[8] Despite an incremental improvement in TAN depletion, an anti-tumor effect was not observed (Figure 4(d,e)) suggesting that reductions in the prevalence of TAN alone does not impede tumor growth. Finally, the anti-tumor effect of anti-Gr1 was recapitulated by G-CSF administration, while TAN prevalence was drastically enhanced (Figure 4(b,c)). Altogether, we conclude TAN depletion *per se* does not impair tumor growth. The common phenotype observed with G-CSF and anti-Gr1 administration suggests that the whole number of TAN is less relevant than their functionality to appreciate the physiology of KP tumors.

RT partially removes TANs but enhances neutrophil homing into tumors

We then investigated the effect of anti-Ly6G when combined with RT, a standard lung cancer treatment. A single clinically relevant[26–28] dose of 11,7 Gy, partially removed TANs, as detected by a BrdU chase (Fig. S4a-d). However, the absolute count of TAN was compensated by day 1.5 as an enhanced recruitment of old CXCR4+ BrdU-60h^{neg} neutrophils (Fig. S4). A reduction of CD62L SiglecF^{neg} TANs was also found after RT

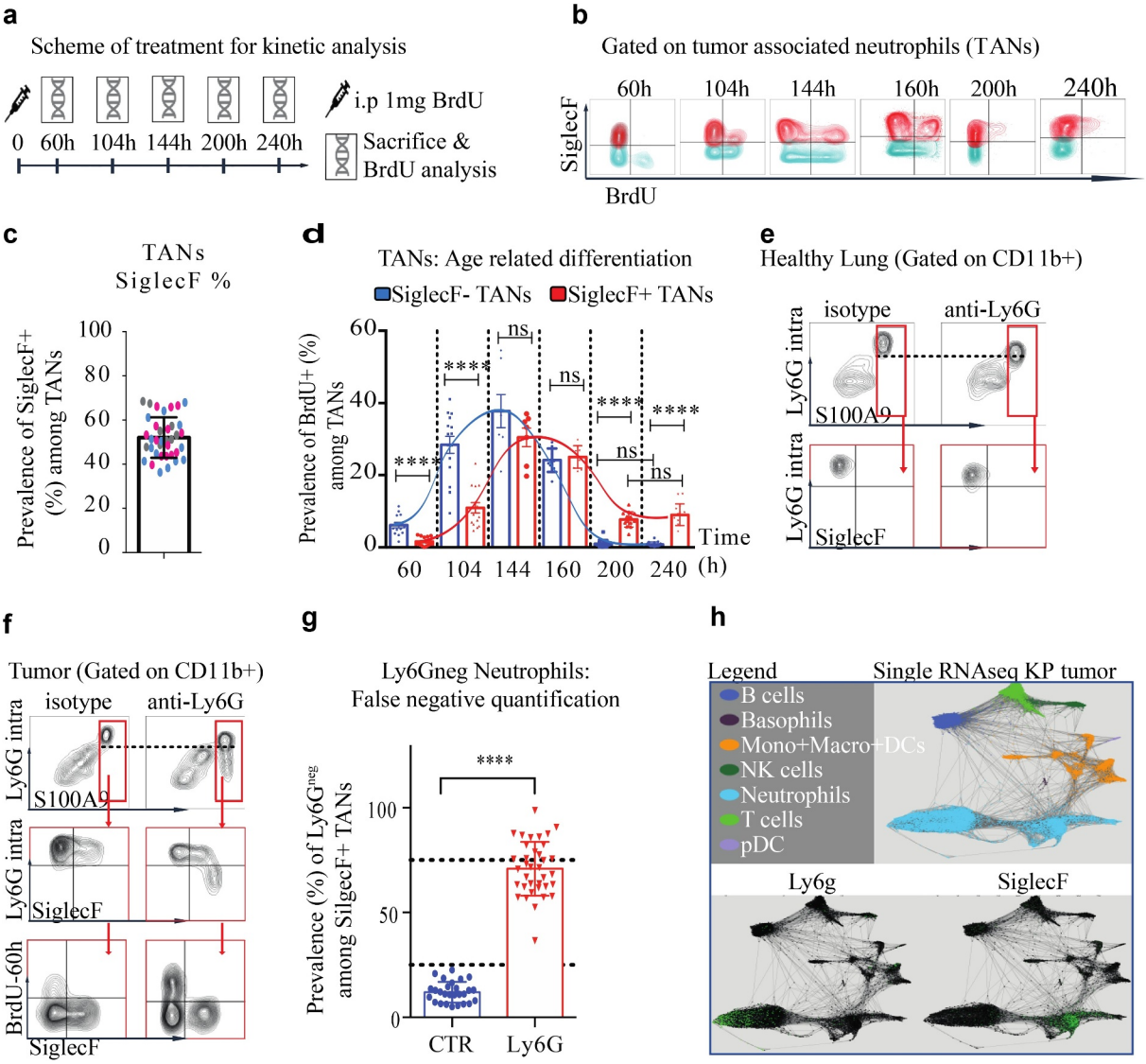

Figure 3. TAN aging enables SiglecF differentiation and depletion resistant Ly6G^{neg} neutrophils. (a). Scheme of treatment: KP mice received 1 mg of BrdU injected i.p (single dose) and sacrificed at dedicated endpoints to correlate neutrophil aging with SiglecF expression. (b). representative FACS plot gated on CD45+ CD11b +Ly6G^{high}F4/80^{neg} SSCa^{low} TANs at each endpoint. (c). SiglecF proportion among all TANs in terminal KP tumor tumors. (Merge of three independent experiments labeled in different colors) (d). TAN BrdU+ fraction according to the SiglecF status from the arrival of BrdU+ TANs 60 h post-BrdU injection, to their extinction 240 post-BrdU injection. Each dot is a quantification of a single tumor. Each endpoint is a single experiment with 4 KP mice per group, 6 to 12 micro-dissected single tumors analyzed. **** $p < 0,0001$ from one-way ANOVA; error bars represent s.d. (e-f). Representative dot plot, gated on CD45+ CD11b+ immune cells, from KP treated for 8 d with anti-Ly6G or relevant isotype CTR. After anti-Ly6G, anti-Ly6G is sensitive to detect S100A9 neutrophils in lungs but not in tumors. (g). Estimation of false negatives upon treatment in old SiglecF^{pos} TANs. **** $p < 0,0001$ from Mann-Whitney test; error bars represent s.d. (h). Differential ly6g expression at the transcriptomic level (data extrapolated from an online single-cell RNA database).

(Fig. S4), compatible with enhanced trans-endothelial migration.[29,30] Additionally, CD62L SiglecF^{neg} TANs exhibited a higher MFI for CXCR4, [23] a marker typically upregulated as neutrophils mature.

RT uncovers the anti-tumor effect of Ly6G-bound residual neutrophils

At the tumor level, RT lowered tumor growth by 50%, but did not elicit tumor regression (Figure 5(a-c)). This result was comparable to various RT treatment schemes published previously,[19,21] using either WTI or stereotactic RT to spare the BM. When anti-Ly6G ab was delivered prior to RT, a partial regression rate of 50% was found 1 month after treatment (Figure 5(a-d)). Data confirmed that RT alone enhanced TAN prevalence among CD45 immune cells 1.5 d after treatment, but not their absolute count, as measured with histological myeloperoxidase staining (Figure 5(e,f) and Fig. S5a-d). After day 1.5 of the anti-Ly6G+RT treatment, an enhanced recruitment of neutrophils both in terms of prevalence and absolute numbers was observed (Figure 5(e,f) and Fig. S5a-d). As opposed to RT alone, the anti-Ly6G+RT combination preferentially enhanced the recruitment of young SiglecF^{neg} BrdU-60h^{pos} neutrophils (Figure 5(g,h)). This latter result suggests that anti-Ly6G accelerates the recruitment of neutrophils after RT. Furthermore, we observed that radiosensitization with anti-

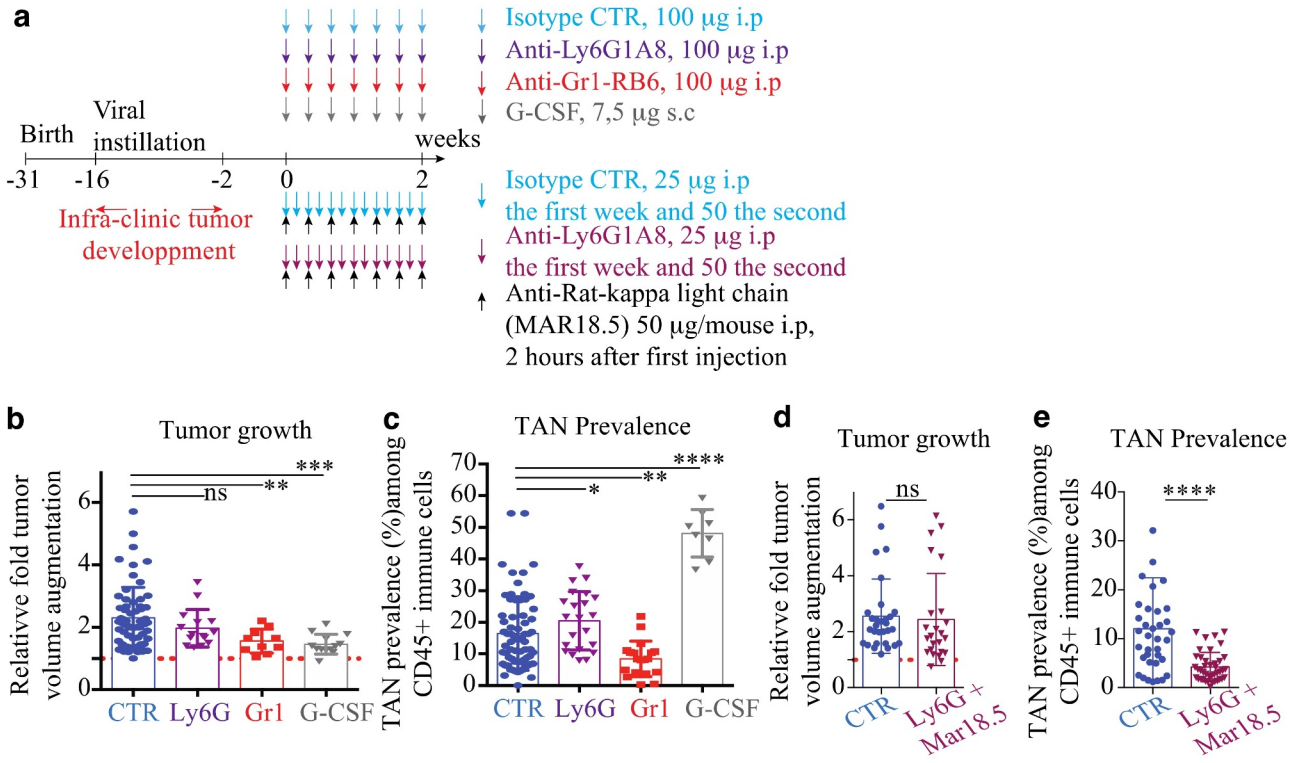

Figure 4. Neutrophil depletion alone has no anti-tumor effect. (a). Experimental design: KP-tumor-bearing mice were exposed for 2 weeks with different treatment regimen affecting neutrophil. Top: anti-Ly6G1A8, anti-Gr1-RB6 were injected i.p every other day (100 µg/mice). G-CSF is injected daily subcutaneously (7,5 µg/mice). Bottom: combination of anti-Ly6G+anti-rat abs to incrementally optimize the killing effect of anti-Ly6G and be comparable to anti-Gr1. Tumor follow-up is performed by CB-CT scan at d0 and d14. Each tumor is contoured using the medical Osirix software and a 3D volume reconstitution is performed. (b): relative to D0 tumor growth after 14 d of treatment. Results obtained from 3 to 7 KP mice per group; (c): TAN prevalence at the end of treatment completion. (d). relative to D0 tumor growth after 14 d of treatment. results obtained from 7 KP mice per group. e.Anti-Ly6G+antirat combination has no anti-tumor effect despite it reduces TANs by >50%. Results from b + c and d + e comes from independent experiment. * $p < .05$, ** $p < .01$, *** $p < 0{,}001$, **** $p < 0{,}0001$ from Mann-Whitney test; error bars represent s.d.

Ly6G was independent from the duration of antibody treatment (Fig. S6a.b). Finally, this effect was partially recapitulated with an adoptive transfer of BM neutrophils pre-incubated with anti-Ly6G, although a lower regression rate was observed in the absence of systemic anti-Ly6G treatment (Fig. S6c.d). Altogether, we conclude that the anti-Ly6G ab intrinsically enhance the anti-tumoral activity of TANs.

Anti-Ly6G mediated radiosensitization is reversed by anti-TNF α administration

To experimentally validate neutrophils can potentiate RT, we administered a single dose of G-CSF 1-hour prior RT, which recapitulated the efficacy of the anti-Ly6G+RT treatment (Figure 5(i)). Given that we found anti-Ly6G bound neutrophils to produce more ROS upon TNFα, together with RNA sequencing data showing that TANs prominently express TNFα receptors, and given that RT leads to the overexpression of TNFα, [31] we decided to investigate directly the role of this cytokine (Figure 5(j-l)). TNF α inhibition consistently abrogated the radiosensitizing effect of anti-Ly6G treatment, demonstrating that anti-Ly6G synergizes with RT through a TNFα-dependent neutrophil gain-of-function.

Discussion

In the present study, we have reported that anti-Ly6G/Ly6G binding and internalization mediates the resistance of neutrophils to depletion. In mice treated with anti-Ly6G, we highlighted the occurrence of $Ly6G^{low}$ neutrophils with ANCAs, a diagnostic feature of granulomatosis with polyangiitis. At a mechanistic level, *in vitro* studies showed anti-Ly6G binding and trafficking potentiated the pro-oxidant activity of neutrophils in response to TNFα. Therefore, while anti-Ly6G is typically used to deplete neutrophils, we investigated whether such a classical strategy actually modified neutrophil biology. In the pre-clinical NSCLC KP-model, we report abnormal neutrophil aging associated with a SiglecF differentiation and a *ly6g* down-regulation. Those cells were prone to depletion resistance. Further, we showed specific reduction of TANs was not sufficient to reduce tumor growth. However, anti-Ly6G administration combined with RT induced a strong and long-lasting tumor regression that was TNF α dependent, while RT alone only slowed tumor growth. Phenotypically, this response was associated with an enhanced homing of anti-Ly6G bound neutrophils to the tumor. Importantly, this acceleration could only be determined on the basis of dynamic measures of newly born neutrophils using BrdU, whereas previous studies generally quantify net yields of neutrophils. Altogether, our data suggest

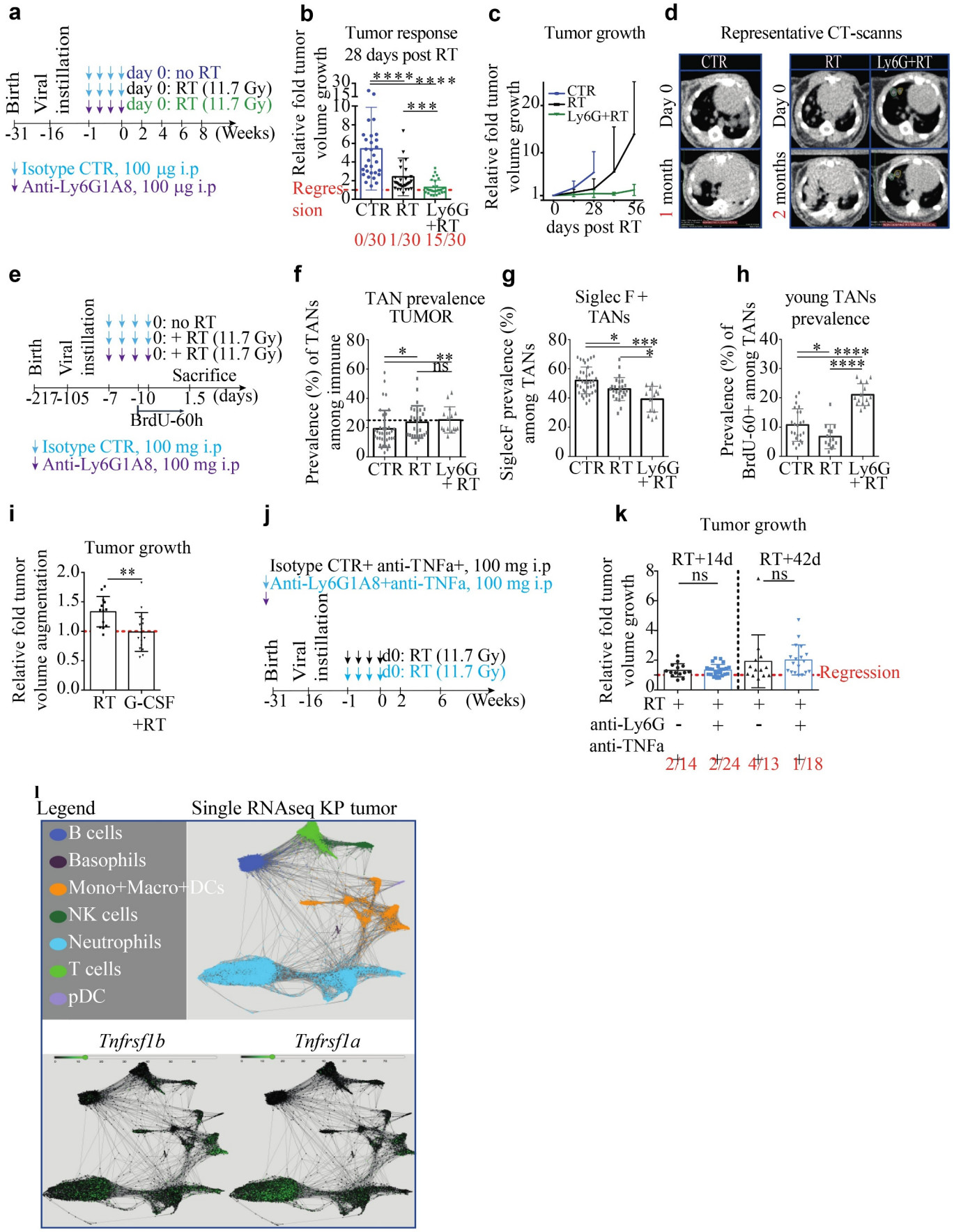

Figure 5. Anti-Ly6G enhances the recruitment of young neutrophils and synergizes with RT. (a). Scheme of treatment: well-established KP tumor-bearing mice received 1 week of isotype/anti-Ly6G ab (100 µg/mice, once every other day), followed by a radiation (RT) treatment at day 0. (b.c). Tumor response is measured as relative growth compared to day 0 by CB-CT scan. Five mice per groups. The number of regressive tumors is given below and indicates regressing tumors. Because untreated mice systematically give rise to escapers and tumor merge, the follow-up had to be stopped after 1 month in CTR group. (d). Illustrative CB-CT scan-based follow up at

indicated endpoints. €. Experimental design to assess early changes after treatment termination in single micro-dissected tumors (f.g.h), each dot is a single micro-dissected tumor). f. TAN prevalence among all immune cells. g. Prevalence of old SiglecF+ TANs among all TANs. h. Prevalence of "young" TANs of 60 hours or less (arrival phase). (i). Because the radiosensitizing effect of anti-Ly6G is associated with an increase of young infiltrating TANs, it suggests a potential gain of function of residual neutrophils. KP mice received a single dose of 7.5 µg of G-CSF one-hour prior RT and tumor growth was assessed as in a. j. Scheme of treatment: well-established KP tumor-bearing mice receive 1 week of anti-TNFα ± anti-Ly6G prior to RT (11.7 Gy). k. 2- and 6-weeks post-RT relative tumor growth: the radiosensitizing effect of anti-Ly6G is not recapitulated in the presence of anti-TNFα. i. Expression of Tnfrsf1b and Tnfrsf1a in KP-TAN (data extrapolated from single-cell RNA sequencing available online). Data from b-c; f-h; i and k are derived from independent experiments with 3 to 7 KP mice per groups. Each dot represents a single tumor. * $p < .05$, ** $p < .01$, *** $p < 0{,}001$, **** $p < 0{,}0001$ from Mann-Whitney test; error bars represent s.d.

an early anti-tumor effect of neutrophils in the KP tumor model, properties that are gradually lost with aging. This work highlights how anti-neutrophil ab therapy can be harnessed further to unleash increased functionality in the fight against cancer.

In cancer patients, neutrophilia is often associated with poor prognosis, [32] which may reflect a multitude of underlying immune-modulated activities. Several approaches are available to modify neutrophil function[33] in efforts to provide mechanistic insight. Genetic neutrophil ablation with Csfr3r knockout mice revealed that TANs impair uterine carcinogenesis by enhancing elimination of hypoxic tumor cells.[34] TAN analysis performed with human primary tumor resections showed they were promoting anti-tumor T cell response in early-stage disease.[34] In mouse Lewis Lung Carcinoma and the spontaneous mammary MMTV-PyMT$^+$ models, genetic ablation of the neutrophil MET proto-oncogene impaired their recruitment and worsened tumor status.[35] In the same PyMT$^+$ model, tail vein infusion of neutrophils reduced the metastatic burden while anti-Ly6G administration increased it.[36] However, the role of neutrophils in the PyMT$^+$ model has been challenged several times using distinct approaches dedicated to promoting neutrophil deficiency, including Gcsf-null background, diphtheria toxin-mediated depletion and anti-Ly6G administration. All these approaches have induced an impairment of the metastatic process in the PyMT$^+$ model. In addition, a subset of IL-17-producing γδ T cells were shown to elicit granulopoiesis and neutrophil polarization, leading to CD8 repression and metastasis enhancement.[5] Interestingly, γδ T cells were since then shown to have low expression of the antioxidant glutathione and to be highly sensitive to neutrophil-derived ROS.[33] Thus, the reported immune-suppressive loop in PyMT may be auto-regulated by neutrophil ROS activation.[33] Collectively, these studies highlight the intricacies, if not confounding impact of neutrophils in cancer, an apparent duality that is recapitulated by the TAN1/TAN2 differentiation paradigm.[37] Interestingly, our work reports that neutrophil aging enables such differentiation.The temporal progression of the neutrophil response is critical to understand their function during infection and inflammation.[38] For instance, upon infection or inflammation, old CXCR4^{pos} neutrophils home faster[39] to the injury site to mitigate threats, while after myocardial lesion, local neutrophil aging results in SiglecF neutrophil differentiation prone to remodeling based on transcriptomic signatures.[40] In the present study, we show for the first time that both paradigms are relevant to the physiology of neutrophils after RT.

Under physiological conditions, neutrophils have an intrinsically short lifespan and are produced at a high rate.[23] We propose that anti-Ly6G binding and internalization maintain newly synthesized neutrophils under a threshold of Ly6G surface expression that impairs depletion. Regardless, neutrophils under anti-Ly6G pressure retain a shorter lifespan than non-treated neutrophils.[8] However, coupled with the enhanced granulopoiesis, a reduced lifespan remains sufficient to rescue neutrophil prevalence. A key finding of our study is that young neutrophils limit tumor growth after RT. Further work is required to clarify the pro-versus anti-tumoral role of older TANs and if/how sequestrated neutrophils may develop an exhausted profile, or passively compete with fresh neutrophil recruitment, thereby losing anti-tumor efficacy.

Some human patients develop anti-neutrophil abs. On one hand, auto-antibodies targeting neutrophil at their surface, such as anti- Human Neutrophil Antigen 1 and 2 (HNA1-2), -CD16/32 and -CD11b are classically associated with primary and secondary auto-immune neutropenia.[41] On the other hand, antibodies targeting intracellular proteins or ANCAs, such as anti-MPO/proteinase3 abs, are associated with vasculitis.[11] How antibodies enter into the neutrophil cytosol is not well understood[11] and models to study ANCAs-related diseases are scarce.[42] Noting that anti-Ly6G treatment did not induce neutropenia but instead generated ANCAs and as given the known severity of ANCA-related disease, the anti-Ly6G may, under specific circumstances, actually activate neutrophil rather than limit their functionality. Furthermore, since Ly6G^{neg} MDSCs have been described previously, and as given the frequently reported limited depleting efficacy of anti-Ly6G ab; it is likely that the present report showing the sequence: 1) neutrophil aging, 2) anti-Ly6G internalization and 3) depletion resistance, 4) neutrophil gain of function; may apply for other inflammatory/cancer models.[24] Finally, given the emerging importance of neutrophil extracellular traps (NETs) in cancer[43] and considering ANCA may intrinsically promote the NET formation, [44,45] it would be interesting to address either administration of anti-Ly6G recapitulates this physiology and to question the role of NET in this primary lung cancer model, especially in the context of radiation-therapy.

To date, anti-Ly6G has been used to induce neutropenia and mimic neutrophil loss of function. Since neutrophil depletion and neutrophil acute activation are functionally antagonistic, a shift in the interpretation of the results is required where the treatment with anti-Ly6G ab would not induce neutrophil depletion but rather "an enhanced turn-over," where neutrophils have a shorter lifespan but a higher production incidence. This scenario enables the following: 1) to integrate young neutrophil anti-tumoral properties; 2) to implement ANCA generation and potential intrinsic activator effects of anti-Ly6G binding; 3) to consider undesirable age-related pro-tumoral differentiation. Realization of these potential opportunities may improve clinical outcomes for cancer patients and provides the rationale for advancing the clinical development of non-depleting anti-neutrophil antibodies.

Material and methods

Animal experiments

Animal experiments were approved by the Swiss (VD2920 and 3242) Ethics Committee for Animal Experimentation and performed within institutional guidelines.

Anti-Ly6G/Gr1 treatments

Anti-Ly6G (BP0075-1), anti-Gr1 (BE0075) and corresponding isotype controls (BP0290 and BP0089) were purchased from BioXcell. Antibodies were injected every other day i.p. Doses and schedule are indicated in Fig. S. An alternative approach with anti-Ly6G+anti-rat kappa Mar18.5 described previously[8] has been additionaly used. For in vitro analysis, BM were collected from untreated C57Bl6 mice and maintained in DMEM. Ex-vivo antibody incubation is performed in 200 µL of PBS with a 10 µg/mL concentration. To avoid cellular interaction, re-incubations at 37° Celsius are performed in 1 mL of PBS under gentle agitation.

Autochthonous mouse model

K-ras$^{LSL\text{-}G12D/WT}$ and *p53*$^{FL/FL}$ mice in a C57BL6/J background purchased from the Jackson Laboratory, bred to obtain *K-ras*$^{LSL\text{-}G12D/WT}$; *p53*$^{FL/FL}$ (KP) mice and provided by E. Meylan's laboratory, (EPFL-Lausanne). KP tumors were initiated upon infection of lung epithelial cells with a lentiviral vector delivering Cre recombinase to activate oncogenic *Kras*^{G12D} and delete *p53* .[22] Thirteen to sixteen-week-old mice were infected intratracheally with 3000 Cre-active lentiviral units.

Irradiation and imaging device

X-ray irradiations were performed using an XRad 225Cx (Pxi Precision X-Ray). The dose prescription was determined at 10 mm depth for a 20 × 20 mm2 field according to previous depth dose measurements in a solid water phantom. Irradiations were performed at 225 keV, 13 mA, with a 0.3 mm copper filter and delivered after fluoroscan imaging to position the mice. Whole thorax irradiation was performed with one vertical beam delivering 11.7 Gy in 256 seconds. During the follow-up period, the tumor volume was monitored once every two weeks starting from the fourteenth-week post-lentiviral instillation. Mice were imaged using the X-rad 225CX irradiator under isoflurane anesthesia. Single tumor volumes were assessed after contouring and reconstruction using the Osirix Lite Software. Treatment groups are randomized and tumor contouring is done blindly. As KP tumors have strong intra and inter-individual heterogeneity,[2] we chose whole thorax radiation (WTI) to limit the number of animals since KP mice require 30 weeks of housing.

Tissue sampling and analysis

For flow cytometry analysis, single-cell suspension was obtained after tissue macro-dissection, following a procedure described previously.[2] A LSRII SORP flow cytometer was used for acquisition. For histological analysis, lungs were gently insufflate with 0.5 mL of 50%PBS-50%OCT (Cell-Path ref 81–0771-00) via the trachea using an I.V surflo catheter (ref SR+OX2225C1). Lobes were separated and OCT-frozen on dry ice. 20 sections of six µm were cut at different depths and then HE stained or stained with appropriated antibodies. Images were obtained with upright microscope Axio Imager.Z1 motorized and analyzed with Zen Zeiss blue software.

G-CSF treatment

Solution of G-CSF was prepared at 250ug/mL of PBS. Mice were subcutaneously injected with 1uL/g daily over 14 d or with a single injection 1 hour prior RT.

BrdU injection and staining procedure

1 mg of BrdU (BD-552598) was injected into mice intraperitoneally at 10 mg/mL in PBS. BrdU labeling was performed according to the provider's protocol. Labeled samples were acquired within 48 hours.

Statistical analysis

All results are disclosed in the main text, as mean±SD. Statistical analysis was performed using nonparametric T-test "Mann-Whitney" using Prism 6 software. Statistical significance is indicated as *p < .05, **p < .01, ***p < .001, ****p < .0001, or ns (not significant).

Main findings

Anti-Ly6G binding and internalization renders neutrophils resistant to depletion

Anti-Ly6G binding primes neutrophils to TNF α-induced oxidative burst

In vivo anti-Ly6G administration generates ANCAs

TAN aging enables N2-like SiglecF^{pos} differentiation

Residual anti-Ly6G bound neutrophils synergize with radiation-therapy

Abbreviations

Antibody (ab); antigen (ag); Granulocyte colony-stimulating factor (G-CSF); Tumor-associated neutrophil (TAN) Radiation Therapy (RT); Bone Marrow (BM); Whole thorax radiation (WTI); anti-neutrophil cytoplasmic antibody (ANCA); Non-small cell lung cancer (NSCLC) Mean Fluorescence Intensity (MFI); Reactive oxygen species (ROS).

Acknowledgments

Animal Facilities of Epalinges for the animal husbandry; Until Flow cytometry, histology and imaging platforms of UNIL for data acquisition. Pr Limoli C for his kind proofreading of the manuscript.

Funding

The study was supported by a grant from ISREC Foundation thanks to Biltema donation. GB was supported by the Nuovo Soldati Foundation and the Swiss National Fund.

ORCID

Romain Vuillefroy de Silly http://orcid.org/0000-0001-6573-9752
Marie-Catherine Vozenin http://orcid.org/0000-0002-2109-8073

Competing interests:

The authors have declared that no conflicts of interest exist.

References

1. Wisdom AJ, Hong CS, Lin AJ, Xiang Y, Cooper DE, Zhang J, Xu ES, Kuo H-C, Mowery YM, Carpenter DJ, et al. Neutrophils promote tumor resistance to radiation therapy. Proc Natl Acad Sci. 2019;116:18584–18589.
2. Faget J, Groeneveld S, Boivin G, Sankar M, Zangger N, Garcia M, Guex N, Zlobec I, Steiner L, Piersigilli A, et al. Neutrophils and snail orchestrate the establishment of a pro-tumor microenvironment in lung cancer. Cell Rep. 2017;21:3190–3204.
3. Engblom C, Pfirschke C, Zilionis R, Da J, Martins S, Bos SA, Courties G, Rickelt S, Severe N, Baryawno N, et al., Osteoblasts remotely supply lung tumors with cancer-promoting SiglecF. Science (2017), doi:10.1126/science.aal5081.
4. Szczerba BM, Castro-giner F, Vetter M, Krol I, Gkountela S, Landin J, Scheidmann MC, Donato C, Scherrer R, Singer J, et al. Neutrophils escort circulating tumour cells to enable cell cycle progression. Nature (2019). doi:10.1038/s41586-019-0915-y.
5. Coffelt SB, Kersten K, Doornebal CW, Weiden J, Vrijland K, Hau C, Verstegen NJM, Ciampricotti M, Hawinkels LJAC. IL17-producing γδ T cells and neutrophils conspire to promote breast cancer metastasis. Nature. 2015;522:345–348.
6. Takeshima T, Pop LM, Laine A, Iyengar P, Vitetta ES, Hannan R. Key role for neutrophils in radiation-induced antitumor immune responses : potentiation with G-CSF. Proc Natl Acad Sci. 2016;1:2–7.
7. Stephens-Romero SD, Mednick AJ, Feldmesser M. The pathogenesis of fatal outcome in murine pulmonary aspergillosis depends on the neutrophil depletion strategy. Infect Immun. 2005;73:114–125.
8. Boivin G, Faget J, Ancey P-B, Gkasti A, Mussard J, Engblom C, Pfirschke C, Contat C, Pascual J, Vazquez J, et al. Durable and controlled depletion of neutrophils in mice. Nat Commun. 2020;11:2762.
9. Vafadarnejad E, Rizzo G, Krampert L, Arampatzi P, Time-resolved single-cell transcriptomics uncovers dynamics of cardiac neutrophil diversity in murine myocardial infarction. (2019).
10. Silliman CC, Fung YL, Bradley Ball J, Khan SY. Transfusion-related acute lung injury (TRALI): current concepts and misconceptions. Blood Rev. 2009;23:245–255.
11. Hilhorst M, Van Paassen P, Tervaert JWC. Proteinase 3-ANCA vasculitis versus myeloperoxidase- ANCA vasculitis. J Am Soc Nephrol. 2015;26:2314–2327.
12. Schernberg A, Nivet A, Dhermain F, Ammari S, Escande A, Pallud J, Louvel G, Deutsch E. Clinical and translational radiation oncology neutrophilia as a biomarker for overall survival in newly diagnosed high-grade glioma patients undergoing chemoradiation. Clin Transl Radiat Oncol. 2018;10:47–52.
13. Schernberg A, Nivet A, Dhermain F, Ammari S, Chargari C, Escande A, Pallud J, Louvel G, Deutsch E. Neutrophilia as a biomarker for overall survival in newly diagnosed high-grade glioma patients from chemoradiation. Int J Radiat Oncol. 2017;99:E106.
14. Schernberg A, Blanchard P, Chargari C, Ou D, Levy A, Gorphe P, Breuskin I, Atallah S, Caula A, Escande A, et al. Leukocytosis, prognosis biomarker in locally advanced head and neck cancer patients after chemoradiotherapy. Clin Transl Radiat Oncol. 2018;12:8–15.
15. Schernberg A, Escande A, Rivin Del Campo E, Ducreux M, Nguyen F, Goere D, Chargari C, Deutsch E. Leukocytosis and neutrophilia predicts outcome in anal cancer. Radiother Oncol. 2017;122:137–145.
16. Caswell DR, Chuang C-H, Yang D, Chiou S-H, Cheemalavagu S, Kim-Kiselak C, Connolly A, Winslow MM. Obligate progression precedes lung adenocarcinoma dissemination. Cancer discov. 2015;85:1–27.
17. Zilionis R, Engblom C, Pfirschke C, Savova V, Zemmour D, Saatcioglu HD, Krishnan I, Maroni G, Meyerovitz CV, Kerwin CM, et al. Single-cell transcriptomics of human and mouse lung cancers reveals conserved myeloid populations across individuals and species. Immunity. 2019;50:e10.
18. Soukup K, Joyce JA. A long-distance relay-tionship between Tumor and Bone. Immunity. 2018;48:13–16.
19. Boivin G, Kalambaden P, Faget J, Rusakiewicz S, Montay-Gruel P, Meylan E, Bourhis J, Lesec G, Vozenin M-C. Cellular composition and contribution of tertiary lymphoid structures to tumor immune infiltration and modulation by radiation therapy. Front Oncol. 2018;8:1–13.
20. Perez BA, Ghafoori AP, Lee C-L, Johnston SM, Li Y, Moroshek JG, Ma Y, Mukherjee S, Kim Y, Badea CT, et al. Assessing the radiation response of lung cancer with different gene mutations using genetically engineered mice. Front Oncol. 2013;3:72.
21. Herter-Sprie GS, Korideck H, Christensen CL, Herter JM, Rhee K, Berbeco RI, Bennett DG. Image-guided radiotherapy platform using single nodule conditional lung cancer mouse models. Nat Commun. 2016;93:292–297.
22. DuPage M, Dooley AL, Jacks T. Conditional mouse lung cancer models using adenoviral or lintiviral delivery of Cre recombinase. Nat Protoc. 2009;4:1064–1072.
23. Adrover JM, Nicolás-Ávila JA, Hidalgo A. Aging: a temporal dimension for neutrophils. Trends Immunol. 2016;37:334–345.
24. Ma C, Greten TF. Editorial: "Invisible" MDSC in tumor-bearing individuals after antibody depletion: fact or fiction? J Leukoc Biol. 2016;99:794.
25. Kirsch DG, Grimm J, Guimaraes AR, Wojtkiewicz GR, Perez BA, Santiago PM, Anthony NK, Forbes T, Doppke K, Weissleder R, et al. Imaging primary lung cancers in mice to study radiation biology. Int J Radiat Oncol. 2010;76:973–977.
26. Taioli E, Lieberman-Cribbin W, Rosenzweig S, van Gerwen MAG, Liu B, Flores RM. Early stage lung cancer survival after wedge resection and stereotactic body radiation. J Thorac Dis. 2018;10:5702–5713.
27. Schonewolf CA, Heskel M, Doucette A, Singhal S, Frick MA, Xanthopoulos EP, Corradetti MN, Friedberg JS, Pechet TT, Christodouleas JP, et al. Five-year long-term outcomes of stereotactic body radiation therapy for operable versus medically inoperable stage i non–small-cell lung cancer: analysis by operability, fractionation regimen, tumor size, and tumor location. Clin Lung Cancer. 2018;20:e63–e71.
28. Katz MS, Husain ZA. Stereotactic radiotherapy or surgery for early-stage non-small-cell lung cancer. Lancet Oncol. 2016;17:e41–e42.
29. Kishimoto TK, Jutila MA, Butcher EC. Identification of a human peripheral lymph node homing receptor: A rapidly down-regulated adhesion molecule. Proc Natl Acad Sci U S A. 1990;87:2244–2248.
30. Filippi MD. Neutrophil transendothelial migration: updates and new perspectives. Blood. 2019;133:2149–2158.
31. Sathishkumar S, Dey S, Meigooni AS, Regine WF, Kudrimoti M, Ahmed MM, Mohiuddin M. The impact of TNF-α induction on therapeutic efficacy following high dose spatially fractionated (GRID) radiation. Technol Cancer Res Treat. 2002;1:141–147.
32. Wu L, Saxena S, Awaji M, Singh RK. Tumor-associated neutrophils in cancer: going pro. Cancers (Basel). 2019:11. doi:10.3390/CANCERS11040564.
33. Mensurado S, Rei M, Lança T, Ioannou M, Gonçalves-Sousa N, Kubo H, Malissen M, Papayannopoulos V, Serre K, Silva-Santos B. Tumor-associated neutrophils suppress pro-tumoral IL-17+ γδ T cells through induction of oxidative stress. PLoS Biol. 2018;16:e2004990.

34. Blaisdell A, Crequer A, Columbus D, Daikoku T, Mittal K, Dey SK, Erlebacher A. Neutrophils oppose uterine epithelial carcinogenesis via debridement of hypoxic tumor cells graphical abstract HHS public access. Cancer Cell. 2015;28:785–799.
35. Finisguerra V, Di Conza G, Di Matteo M, Serneels J, Costa S, Thompson AAR, Wauters E, Walmsley S, Prenen H, Granot Z, et al. MET is required for the recruitment of anti-tumoural neutrophils. Nature. 2015;522:349–353.
36. Granot Z, Henke E, Comen EA, King TA, Norton L, Benezra R. Tumor entrained neutrophils inhibit seeding in the premetastatic lung. Cancer Cell. 2011;20:300–314.
37. Fridlender ZG, Sun J, Kim S, Kapoor V, Cheng G, Worthen GS, Albelda SM. Polarization of tumor-associated neutrophil (TAN) phenotype by TGF-β: "N1" versus "N2" TAN. Cancer. 2010;16:183–194.
38. Reglero-real N, Leukocyte Trafficking : time to Take Time Seriously, 273–275 (2019).
39. Uhl B, Vadlau Y, Zuchtriegel G, Nekolla K, Sharaf K, Gaertner F, Massberg S, Krombach F, Reichel CA. Aged neutrophils contribute to the first line of defense in the acute inflammatory response. Blood. 2018;128:2327–2338.
40. Vafadarnejad E, Rizzo G, Krampert L, Arampatzi P, Nugroho VA, Schulz D, Roesch M, Alayrac P, Vilar J, Silvestre J-S, et al., Time-resolved single-cell transcriptomics uncovers dynamics of cardiac neutrophil diversity in murine myocardial infarction. *bioRxiv*, 738005 (2019).
41. Grayson PC, Sloan JM, Niles JL, Monach PA, Merkel PA. Antineutrophil cytoplasmic antibodies, autoimmune neutropenia, and vasculitis. Semin Arthritis Rheum. 2011;41:424–433.
42. Little MA, Al-Ani B, Ren S, Al-Nuaimi H, Leite M, Alpers CE, Savage CO, Duffield JS. Anti-proteinase 3 anti-neutrophil cytoplasm autoantibodies recapitulate systemic vasculitis in mice with a humanized immune system. PLoS One. 2012:7. doi:10.1371/journal.pone.0028626.
43. Vorobjeva NV, Chernyak BV. NETosis: molecular mechanisms, role in physiology and pathology. Biochem. 2020;85:1178–1190.
44. Lee KH, Kronbichler A, Park DDY, Park YM, Moon H, Kim H, Choi JH, Choi YS, Shim S, Lyu IS, et al. Neutrophil extracellular traps (NETs) in autoimmune diseases: A comprehensive review. Autoimmun Rev. 2017;16:1160–1173.
45. Nakazawa D, Masuda S, Tomaru U, Ishizu A. Pathogenesis and therapeutic interventions for ANCA-associated vasculitis. Nat Rev Rheumatol. 2019;15:91–101.